Monthly Notices
of the
ROYAL ASTRONOMICAL SOCIETY

MNRAS **475,** L30–L34 (2018) doi:10.1093/mnrasl/slx208
Advance Access publication 2018 January 5

Phosphorus-bearing molecules in the Galactic Center

V. M. Rivilla,[1★] I. Jiménez-Serra,[2] S. Zeng,[2] S. Martín,[3,4] J. Martín-Pintado,[5] J. Armijos-Abendaño,[6] S. Viti,[7] R. Aladro,[8] D. Riquelme,[8] M. Requena-Torres,[9] D. Quénard,[2] F. Fontani[1] and M. T. Beltrán[1]

[1]*INAF/Osservatorio Astrofisico di Arcetri, Largo Enrico Fermi 5, I-50125 Florence, Italy*
[2]*School of Physics and Astronomy, Queen Mary University of London, Mile End Road, London E1 4NS, UK*
[3]*Joint ALMA Observatory, Alonso de Córdova 3107, Vitacura 763 0355, Santiago, Chile*
[4]*European Southern Observatory, Alonso de Córdova 3107, Vitacura Casilla 763 0355, Santiago, Chile*
[5]*Centro de Astrobiología (INTA-CSIC), Ctra. de Ajalvir Km. 4, Torrejón de Ardoz, E-28850 Madrid, Spain*
[6]*Observatorio Astronómico de Quito, Escuela Politécnica Nacional, Av. Gran Colombia S/N y Av. Diez de Agosto, Quito 170403, Ecuador*
[7]*Department of Physics and Astronomy, UCL, Gower St., London WC1E 6BT, UK*
[8]*Max-Planck-Institut für Radioastronomie, Auf dem Hügel 69, D-53121 Bonn, Germany*
[9]*Space Telescope Science Institute, 3700 San Martin Drive, Baltimore, MD 21218, USA*

Accepted 2017 December 19. Received 2017 November 28; in original form 2017 November 3

ABSTRACT

Phosphorus (P) is one of the essential elements for life due to its central role in biochemical processes. Recent searches have shown that P-bearing molecules (in particular PN and PO) are present in star-forming regions, although their formation routes remain poorly understood. In this letter, we report observations of PN and PO towards seven molecular clouds located in the Galactic Center, which are characterized by different types of chemistry. PN is detected in five out of seven sources, whose chemistry is thought to be shock-dominated. The two sources with PN non-detections correspond to clouds exposed to intense UV/X-rays/cosmic ray (CR) radiation. PO is detected only towards the cloud G+0.693−0.03, with a PO/PN abundance ratio of ∼1.5. We conclude that P-bearing molecules likely form in shocked gas as a result of dust grain sputtering, while are destroyed by intense UV/X-ray/CR radiation.

Key words: ISM: abundances – ISM: clouds – ISM: molecules – Galaxy: Centre.

1 INTRODUCTION

Phosphorus (P) is essential for life because it plays a central role in the formation of macromolecules such as phospholipids (the structural components of cellular membranes) and the deoxyribonucleic acid (DNA; Maciá, Hernández & Oró 1997). It is synthesized in massive stars (Koo et al. 2013), and it has relatively low cosmic abundance relative to hydrogen (2.8×10^{-7}; Grevesse & Sauval 1998). It is believed to be heavily depleted in cold and dense molecular clouds (Turner et al. 1990; Wakelam & Herbst 2008). Until recently, only a few simple P-bearing species (PN, PO, CP, HCP, C_2P, and PH_3) had been identified towards the envelopes of evolved stars (Tenenbaum, Woolf & Ziurys 2007; De Beck et al. 2013; Agúndez et al. 2014). Among the detected P-bearing molecules, PN and PO are the only ones that have been reported in star-forming regions. For decades, PN remained as the only P-bearing species observed in these regions (Turner & Bally 1987; Ziurys 1987; Yamaguchi et al. 2011; Fontani et al. 2016), while PO has been discovered just recently in the surroundings of both high- and low-mass protostars (with PO/PN abundance ratios of ∼1–3; Lefloch et al. 2016; Rivilla et al. 2016).

Three routes have been proposed for the formation of PN and PO in star-forming regions: (i) shock-induced desorption of P-bearing species (e.g. PH_3) from dust grains and subsequent gas-phase formation (Aota & Aikawa 2012; Lefloch et al. 2016); (ii) high-temperature gas-phase chemistry after the thermal desorption of PH_3 from ices (Charnley & Millar 1994); and (iii) gas-phase formation of PN and PO during the cold collapse phase and subsequent thermal desorption (at temperatures ≥35 K) by protostellar heating (Rivilla et al. 2016). Due to the limited number of observations available, and the limited range of physical conditions of the observed regions with detected P-bearing molecules, the formation routes for PN and PO are strongly debated.

In this letter, we present observations of PN and PO towards seven regions spread across the Central Molecular Zone (CMZ) in the Galactic Center (GC). These sources are excellent laboratories to test the chemistry of P-bearing molecules since they

★ E-mail: rivilla@arcetri.astro.it

Published by Oxford University Press on behalf of the Royal Astronomical Society

Table 1. Sample and results.

Source	RA (J2000) (h m s)	Dec. (J2000) (° ′ ″)	Type[a]	Vel. (km s^{-1})	FWHM (km s^{-1}) PN	^{29}SiO	N ($\times 10^{12}$ cm^{-2}) N(PN)	N(PO)	N(^{29}SiO)	N(C^{34}S)[(b)]	[PO/PN]	T$_{ex}$(K) PN	^{29}SiO
G+0.693−0.03	17 47 21.86	−28 21 27.14	Shock	69	24.0	24.2	5.6 ± 0.3	8 ± 3	15.5 ± 0.7	50 ± 7	1.5 ± 0.4	≤6.3	6.8 ± 0.4[c]
S+0.24+0.01	17 46 09.86	−28 43 42.39	Shock	34	12.0	21.8	4.8 ± 0.5	<13	11.7 ± 0.2	35 ± 2	<2.7	≤4.2	6.3 ± 0.8[c]
M−0.02 −0.07	17 45 50.64	−28 59 08.81	Shock	47	19.0	27.0	4.7 ± 0.8	<15	33.9 ± 0.7	87 ± 5	<3.1	5.0[d]	4.7 ± 0.5[c]
SgrB2 N	17 47 20.39	−28 22 19.25	Shock	64	6.7	6.6	6 ± 1	<19	67.6 ± 0.8	98 ± 14	<1.8	5.0[d]	5.0[d]
				82	9.0	9.0	11 ± 1	<19	51.3 ± 0.6	26 ± 8	<3.2	5.0[d]	5.0[d]
SgrB2 M	17 47 20.41	−28 23 07.25	Shock	60	6.7	6.5	9.3 ± 0.7	<63	63 ± 10	129 ± 22	<6.8	5.0[d]	5.0[d]
				66	11.4	10.1	18.2 ± 0.9	<63	178 ± 22	58 ± 13	<3.5	5.0[d]	5.0[d]
M+0.02−0.02	17 45 42.71	−28 55 50.98	Rad.	93	–	32	<0.7	<11	4.9 ± 0.8	25 ± 6	–	5.0[d]	6.0 ± 0.9[c]
				−5.0	–	32	<0.7	<11	3.8 ± 0.4	34 ± 15	–	5.0[d]	6.0[d]
SgrA*(−30 arcsec,	17 45 37.74	−29 00 58.18	Rad.	20	–	–	<0.7	<18	<2.1	54 ± 15	–	5.0[d]	5.0[d]
−30 arcsec)			Rad.	−70	–	–	<0.7	<18	<2.1	–[e]	–	5.0[d]	5.0[d]

Notes. [a]Shock: Clouds with shock-dominated chemistry; Rad.: Clouds with radiation-dominated chemistry. [b]Values extracted from Martín et al. (2008) (see their table 4) for all sources except for SgrB2 N and M (see the text). [c]The MADCUBA-AUTOFIT was performed using simultaneously the ^{29}SiO (2−1), (3−2), and (4−3) transitions. [d]Value fixed. [e]Not derived in Martín et al. (2008).

show different physical properties (high kinetic temperatures, low dust temperatures, and moderate densities) and chemistries dominated by either UV photons, cosmic rays (CRs), X-rays, or shock waves.

2 THE SAMPLE

The CMZ (Morris & Serabyn 1996) of the GC harbours the most chemically rich regions in the Galaxy (Martín-Pintado et al. 2001). The physical conditions in the CMZ are very different from those found in the Galactic disc with high gas temperatures (≥60–100 K), low dust temperatures (≤20 K), and low H_2 gas densities (∼10^4 cm^{-3}; Rodríguez-Fernández et al. 2000; Güesten & Philipp 2004; Ginsburg et al. 2016). Since dust is too cold for the evaporation of ices, it has been proposed that the observed chemical richness is due to grain sputtering in widespread, low-velocity shocks (Martín-Pintado et al. 1997). In addition, depending on their location, the clouds in the CMZ may be exposed to intense UV radiation (photon-dominated regions or PDRs), X-rays, and/or CRs, which strongly affect the chemistry of these clouds (Martín et al. 2008). Our selected sample includes two different types of sources (see Table 1):

(i) Shock-dominated regions: G+0.693−0.03, S+0.24+0.01, M−0.02 −0.07, and the molecular rich envelopes of SgrB2 N and M. The first two sources do not show evidence of ongoing star formation, while the last three are associated with massive protoclusters (de Vicente et al. 2000; Belloche et al. 2013; Sánchez-Monge et al. 2017). In all these regions, SiO is largely enhanced due to shocks (Martín et al. 2008).

(ii) Radiation-dominated regions: SgrA* [offset (−30 arcsec, −30 arcsec)] and M+0.02−0.02. The first is located at the inner edge of the circumnuclear disc, 1.5 pc away from the black hole. Its molecular gas is strongly affected by the UV/X-ray radiation (Amo-Baladrón, Martín-Pintado & Martín 2011; Harada et al. 2014). The CR ionization rate in this region is enhanced by several orders of magnitude (Goto et al. 2008), causing a similar effect on the chemistry as that produced by UV photons (Harada et al. 2015). M+0.02−0.02 is a very compact cloud whose chemistry is thought to be affected by UV radiation and enhanced CR ionization rate (Martín et al. 2008), and also by X-rays (Ponti et al. 2010).

Table 2. PN, PO, ^{29}SiO, and C^{34}S transitions used in this work.

Molecule	Transition	Frequency (GHz)	E$_{up}$ (K)	A$_{ul}$ (s^{-1})
PN	2−1	93.979 77	6.8	2.9×10^{-5}
PN	3−2	140.967 69	13.5	1.1×10^{-4}
PO	F=3−2, l=e[a]	108.998 45	8.4	2.1×10^{-5}
PO	F=2−1, l=e[a]	109.045 40	8.4	1.9×10^{-5}
PO	F=3−2, l=f[a]	109.206 20	8.4	2.1×10^{-5}
PO	F=2−1, l=f[a]	109.281 19	8.4	1.9×10^{-5}
^{29}SiO	2−1	85.759 20	6.2	2.8×10^{-5}
^{29}SiO	3−2	128.636 71	12.3	1.0×10^{-4}
^{29}SiO	4−3	171.512 29	20.6	2.5×10^{-4}
C^{34}S	2−1	96.412 95	6.3	1.6×10^{-5}
C^{34}S	3−2	144.617 10	11.8	5.8×10^{-5}
C^{34}S	5−4	241.016 09	27.0	2.8×10^{-4}

Notes. [a]J=5/2→3/2, Ω=1/2 quadruplet.

3 OBSERVATIONS

The observations were conducted in multiple sessions between 2003 and 2009. The observed positions for all sources are listed in Table 1. In the 2003–2005 sessions, the SIS C and D receivers covered the 2 mm window (128–176 GHz), whilst between 2009 and 2011 the broad-band EMIR receivers (Carter et al. 2012) were used at 3 mm (80–116 GHz). The spectral resolution was in the range 6.8 –9.3 km s^{-1} which was high enough to resolve the lines profiles of ∼20 km s^{-1}. The molecular transitions studied in this work are shown in Table 2. Since it is well known that the molecular emission towards these sources is extended over the beam (Requena-Torres et al. 2006; Martín et al. 2008), in our analysis we have used the line intensities measured in units of antenna temperature, T_A^*, as we did in Martín et al. (2008) and Requena-Torres, Martín-Pintado & Morris (2008). To complete the sample, we also used the publicly available 3 mm spectral survey obtained towards SgrB2 N and M by Belloche et al. (2013).

4 ANALYSIS AND RESULTS

PN (2−1) was detected towards all the shock-dominated clouds in our sample (see Fig. 1 and Table 1). In the case of SgrB2 N and M, PN (2−1) was detected in absorption against the bright continuum emission of the hot molecular cores and compact H II regions, indicating its presence within the low-density envelope of SgrB2. PN

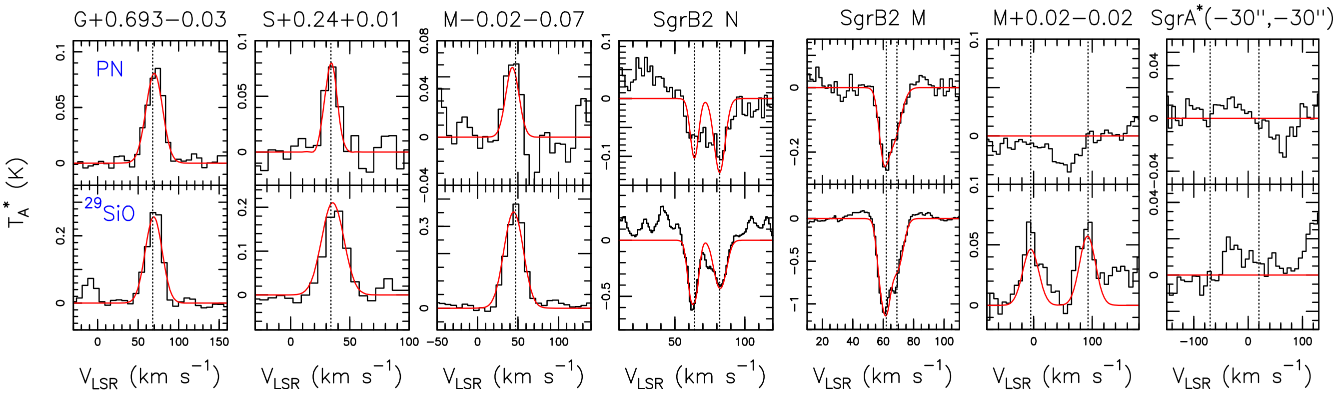

Figure 1. PN (2−1) and ^{29}SiO (2−1) lines measured towards all sources. The LTE best fits from MADCUBA are also shown (red lines).

was not detected towards the radiation-dominated sources: SgrA* (−30 arcsec,−30 arcsec) and M+0.02−0.02. In both sources, we have searched at the two velocity components found by Martín et al. (2008) in other molecular tracers (see Table 1). PN (3−2) was not detected towards any source.

To derive the column densities of the molecular species across our sample, we have used MADCUBA,[1] which produces synthetic spectra assuming Local Thermodynamic Equilibrium (LTE) conditions. First, we fixed manually the FWHM and the velocity of the lines to values that reproduce well the observed lines (see Table 1). Then, we used the MADCUBA−AUTOFIT tool, which compares the synthetic LTE spectra with the observed spectra and provides the best non-linear least-squared fit using the Levenberg–Marquardt algorithm. We run AUTOFIT to fit simultaneously the PN (2−1) detections and the (3−2) non-detections. The algorithm converged for G+0.693−0.03 and S+0.24+0.01, and found low temperatures of 6.3 and 4.2 K, respectively. We note that these excitation temperatures should be considered as upper limits since higher values of T_{ex} would excite the PN(3−2) transition, which was not detected.

For M−0.02−0.07, the AUTOFIT algorithm did not converge, and thus T_{ex} was fixed to 5 K. The derived values for the PN column densities derived with AUTOFIT are shown in Table 1. The low T_{ex} found are similar to those observed for other species in these clouds (∼5–15 K; Martín et al. 2008; Requena-Torres et al. 2008), and to those recently found for PN in several massive cores in the Galactic disc (Mininni et al., submitted). The most likely explanation for the T_{ex} found, much lower than the kinetic temperatures, is that PN is subthermally excited due to the relatively low H_2 densities (∼10^4 cm^{-3}; Güsten & Philipp 2004) compared with the critical densities of PN (>10^5 cm^{-3}; Toboła et al. 2007).

The PN absorption lines towards SgrB2 N and M were fitted assuming that the PN gas is located in a foreground layer with T_{ex} = 5 K, and considering that the SgrB2 N and M hot cores are background blackbody emitters with sizes of 2 arcsec and gas temperatures of 150 K (Belloche et al. 2013; Sánchez-Monge et al. 2017). The PN absorption shows two different velocity components (Fig. 1) that have been fitted simultaneously.

PN was not detected towards the radiation-dominated regions, SgrA* (−30 arcsec,−30 arcsec) and M+0.02−0.02, and then we derived the 3σ upper limits for the column density.

[1] Madrid Data Cube Analysis (MADCUBA) is a software developed in the Center of Astrobiology (Madrid) to visualize and analyse single spectra and data cubes (Rivilla et al. 2017a,b).

We have also searched for the PO quadruplet at ∼109 GHz (Table 2). PO has only been detected towards G+0.693−0.03, known to be rich in O-bearing molecules (Requena-Torres et al. 2006, 2008). Fig. 2 shows the PO detection compared to that reported by Rivilla et al. (2016) towards the hot core W51 e1/e2. The PO lines were fitted assuming T_{ex} = 6.3 K, that inferred from PN. The derived [PO/PN] ratio is ∼1.5, similar to that measured in star-forming regions (Lefloch et al. 2016; Rivilla et al. 2016). For the other sources (with PO non-detections), we computed the upper limits of the PO column density considering the same T_{ex} assumed for PN. In all cases, the [PO/PN] ratio is <7 (Table 1).

To test whether the chemistry of P-bearing molecules is indeed correlated with the presence of shocks, we have also analysed the emission of the shock tracer SiO. Since the main isotopologue is optically thick across the GC, we have used the optically thinner isotopologue ^{29}SiO. By simultaneously fitting the (2−1), (3−2), and (4−3) transitions of this molecule, we have found T_{ex} in the range 4.7–6.8 K for G+0.693−0.03, S+0.24+0.01, M−0.02 −0.07, and M+0.02−0.02. In contrast, this species is not detected in none of the velocity components of SgrA* (−30 arcsec,−30 arcsec) and we have thus computed the upper limits. For SgrB2 N and M, the ^{29}SiO (2−1) emission is seen in absorption (Fig. 1) and, as for PN, we have considered two velocity components and a fixed T_{ex} = 5 K to compute the column densities (Table 1).

In Fig. 3, we plot the column density ratios PN/C^{34}S versus those obtained for ^{29}SiO/C^{34}S. The optically thin C^{34}S isotopologue is used here because it is a good proxy of the H_2 column density, as shown by Requena-Torres et al. (2006) in a survey of GC clouds. CS is also a good reference to compute relative molecular ratios because its chemistry is nearly independent of the physical properties of the sources: i) unlike other species (such as CH_3OH or HNCO), it is barely enhanced in shocked-gas (Requena-Torres et al. 2006); and ii) it is photoresistant, so it is expected to survive in PDRs (Requena-Torres et al. 2006; Martín et al. 2008).

For G+0.693−0.03, S+0.24+0.01, M−0.02 −0.07, SgrA* (−30 arcsec,−30 arcsec), and M+0.02−0.02, we have used the C^{34}S column densities obtained from C^{34}S (3−2) and C^{34}S (5−4) by Martín et al. (2008). For SgrB2 N and M, Martín et al. (2008) did not consider the two velocity components used in our analysis, and therefore, we have re-done the analysis. For SgrB2 N, we have used C^{34}S (2−1). For SgrB2 M, the C^{34}S (2−1) line presents strong emission blended with the absorption feature and therefore, we used the C^{34}S (3−2) transition instead. We used the T_{ex} from Martín et al. (2008), to be consistent with the other sources. For completeness, in the case of sources with no detection

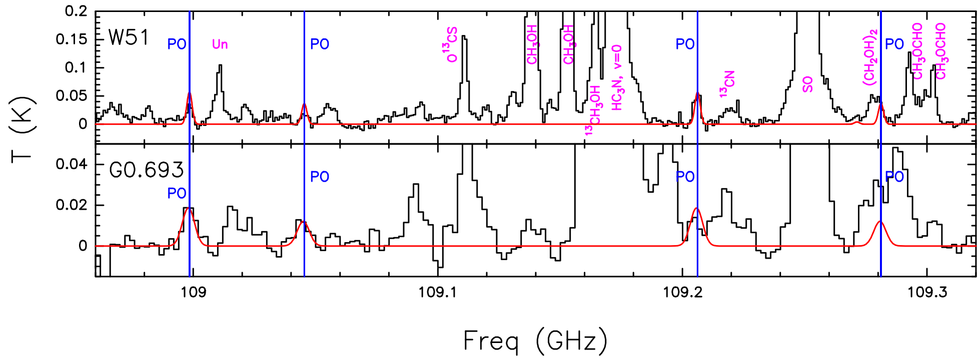

Figure 2. PO detection towards G+0.693-0.03 (lower panel) compared with the detection towards the hot molecular core W51 e1/e2 from Rivilla et al. (2016) (upper panel). The PO quadruplet is shown with vertical blue lines. Other molecular species are labelled in the upper panel. The MADCUBA-fitted LTE synthetic spectrum of PO in both sources is shown with red lines.

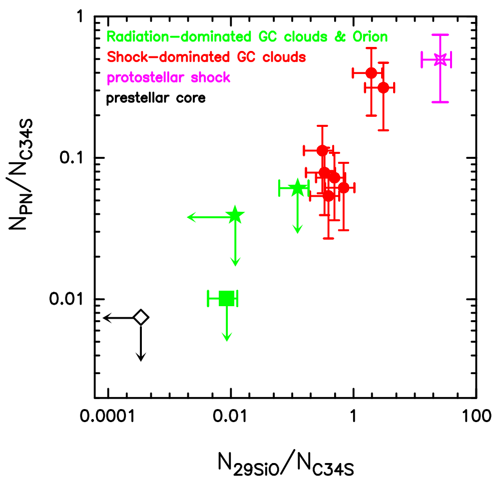

Figure 3. Column density ratios of PN and ^{29}SiO with respect to C^{34}S. The different types of sources are shock-dominated GC clouds (red dots) and radiation-dominated GC regions (green stars). The values obtained towards the Orion Bar (a prototypical PDR, green square; Cuadrado, private communication), the L1157-B1 shock (magenta open star), and the L1544 pre-stellar core (black open diamond; from the data set from Jiménez-Serra et al. 2016) have also been added. Arrows indicate 3σ upper limits. The error bars correspond to conservative uncertainties of ± half of the molecular ratio value.

of PN or ^{29}SiO, we have plotted in Fig. 3 the values of the upper limits.

Fig. 3 reveals that there is a positive trend between PN and ^{29}SiO abundances. Although our upper limits towards the PDR-like sources do not allow us to confirm a correlation between PN and ^{29}SiO, these two species seem to show a similar behaviour: the PN detections correspond to the ^{29}SiO-rich sources, while PN is not present towards those sources with weaker ^{29}SiO. This strongly suggests that PN is enhanced by shocks. This conclusion is in good agreement with the results found by Mininni et al. (submitted) in some massive dense cores of the Galactic disc, and with the shock modelling results from Lefloch et al. (2016), which proposed that PN is formed in gas phase after the shock-induced desorption of PH_3. Since PN is not detected in any GC radiation-dominated cloud, this molecule is likely dissociated by the intense UV/X-ray/CR radiation, similarly to HNCO and CH_3OH (Martín et al. 2008). For completeness, in Fig. 3, we also add the PN/C^{34}S and ^{29}SiO/C^{34}S column density ratios measured towards the shocked region L1157-B1 (Bachiller & Pérez Gutiérrez 1997; Lefloch et al. 2016; Podio et al. 2017), the Orion Bar (a prototypical PDR; Cuadrado et al. 2015; Cuadrado, private communication), and L1544 (a pre-stellar core without any sign of star formation activity; Ward-Thompson, Motte & Andre 1999). In the latter two cases, the ^{29}SiO column density was calculated from SiO assuming ^{28}Si/^{29}Si = 19.6 (Wilson 1999). For L1544, the molecular column densities were calculated using $T_{ex} = 5$ K. The column density ratios derived for these regions nicely follow the trend observed for the GC clouds: PN is well correlated with ^{29}SiO in the L1157-B1 shock while it remains undetected in the PDR. Since PN is not detected in the L1544 pre-stellar core either, this implies that P, like Si, is heavily depleted in molecular dark clouds, in agreement with the shock modelling results from Lefloch et al. (2016), and with observations in molecular dark clouds (Turner et al. 1990).

5 CONCLUSIONS

We searched for P-bearing molecules PN and PO towards seven clouds located in the GC, known to present different types of chemistry. PN is detected towards five of the seven sources, and PO is detected only towards one of the sources, G+0.693−0.03, which is thought to be the richest source of O-bearing molecules in the GC. The derived PO/PN abundance ratio is 1.5, similar to values previously found in star-forming regions. The regions where P-bearing species have been detected are clouds thought to be affected by shock waves, and rich in the well-known shock tracer ^{29}SiO. The two sources where no P-bearing molecules were detected are regions exposed to intense radiation, and exhibit lower abundances of ^{29}SiO. We thus conclude that P-bearing species are formed in the gas phase after the shock-induced sputtering of the grain mantles, and that they are efficiently destroyed by the high CRs/X-rays/UV-photon radiation expected in some regions of the GC.

ACKNOWLEDGEMENTS

We thank S. Cuadrado and J. Goicoechea for sharing their data on the Orion bar. VMR is funded by the H2020 programme under the MSC grant agreement no. 664931. IJ-S and DQ acknowledge the financial support received from the STFC through an ER Fellowship and Grant (ST/L004801 and ST/M004139). JM-P acknowledges support by the MINECO grants ESP2013-47809-C03-01 and ESP2015-65597-C4-1. SZ acknowledges support through a Principal's studentship funded by QMUL. DR acknowledges support of the Collaborative Research Council 956, subproject A5, funded by the DFG.

REFERENCES

Agúndez M., Cernicharo J., Decin L., Encrenaz P., Teyssier D., 2014, ApJ, 790, L27
Amo-Baladrón M. A., Martín-Pintado J., Martín S., 2011, A&A, 526, A54
Aota T., Aikawa Y., 2012, ApJ, 761, 74
Bachiller R., Pérez Gutiérrez M., 1997, ApJ, 487, L93
Belloche A., Müller H. S. P., Menten K. M., Schilke P., Comito C., 2013, A&A, 559, A47
Carter M. et al., 2012, A&A, 538, A89
Charnley S. B., Millar T. J., 1994, MNRAS, 270, 570
Cuadrado S., Goicoechea J. R., Pilleri P., Cernicharo J., Fuente A., Joblin C., 2015, A&A, 575, A82
De Beck E., Kamiński T., Patel N. A., Young K. H., Gottlieb C. A., Menten K. M., Decin L., 2013, A&A, 558, A132
de Vicente P., Martin-Píntado J., Neri R., Colom P., 2000, A&A, 361, 1058
Fontani F., Rivilla V. M., Caselli P., Vasyunin A., Palau A., 2016, ApJ, 822, L30
Ginsburg A. et al., 2016, A&A, 586, A50
Goto M. et al., 2008, ApJ, 688, 306
Grevesse N., Sauval A. J., 1998, Space Sci. Rev., 85, 161
Güesten R., Philipp S., 2004, 91, 253
Güsten R., Philipp S. D., 2004, in Pfalzner S., Kramer C., Staubmeier C., Heithausen A., eds, Vol. 91, The Dense Interstellar Medium in Galaxies. Springer, Berlin, p. 253
Harada N., Riquelme D., Viti S., Menten K., Requena-Torres M., Güsten R., Hochgürtel S., 2014, in Sjouwerman L. O., Lang C. C., Ott J., eds, IAU Symp. Vol. 303, The Galactic Center: Feeding and Feedback in a Normal Galactic Nucleus. Kluwer, Dordrecht, p. 78
Harada N. et al., 2015, A&A, 584, A102
Jiménez-Serra I. et al., 2016, ApJ, 830, L6
Koo B.-C., Lee Y.-H., Moon D.-S., Yoon S.-C., Raymond J. C., 2013, Science, 342, 1346
Lefloch B. et al., 2016, MNRAS, 462, 3937
Maciá E., Hernández M. V., Oró J., 1997, Orig. Life Evol. Biosph., 27, 459
Martín S., Requena-Torres M. A., Martín-Pintado J., Mauersberger R., 2008, ApJ, 678, 245
Martín-Pintado J., de Vicente P., Fuente A., Planesas P., 1997, ApJ, 482, L45
Martín-Pintado J., Rizzo J. R., de Vicente P., Rodríguez-Fernández N. J., Fuente A., 2001, ApJ, 548, L65
Morris M., Serabyn E., 1996, Annu. Rev. Astron. Astrophys., 34, 645
Podio L. et al., 2017, MNRAS, 470, L16
Ponti G., Terrier R., Goldwurm A., Belanger G., Trap G., 2010, ApJ, 714, 732
Requena-Torres M. A., Martín-Pintado J., Rodríguez-Franco A., Martín S., Rodríguez-Fernández N. J., de Vicente P., 2006, A&A, 455, 971
Requena-Torres M. A., Martín-Pintado J. S. M., Morris M. R., 2008, ApJ, 672, 352
Rivilla V. M., Fontani F., Beltrán M. T., Vasyunin A., Caselli P., Martín-Pintado J., Cesaroni R., 2016, ApJ, 826, 161
Rivilla V. M., Beltrán M. T., Cesaroni R., Fontani F., Codella C., Zhang Q., 2017a, A&A, 598, A59
Rivilla V. M., Beltrán M. T., Martín-Pintado J., Fontani F., Caselli P., Cesaroni R., 2017b, A&A, 599, A26
Rodríguez-Fernández N. J., Martín-Pintado J., de Vicente P., Fuente A., Huettemeister S., Wilson T. L., Kunze D., 2000, A&A, 356, 695
Sánchez-Monge A. et al., 2017, A&A, 604, A6
Tenenbaum E. D., Woolf N. J., Ziurys L. M., 2007, ApJ, 666, L29
Toboła R., Kłos J., Lique F., Chałasiński G., Alexander M. H., 2007, A&A, 468, 1123
Turner B. E., Bally J., 1987, ApJ, 321, L75
Turner B. E., Tsuji T., Bally J., Guelin M., Cernicharo J., 1990, ApJ, 365, 569
Wakelam V., Herbst E., 2008, ApJ, 680, 371
Ward-Thompson D., Motte F., Andre P., 1999, MNRAS, 305, 143
Wilson T. L., 1999, Rep. Prog. Phys., 62, 143
Yamaguchi T. et al., 2011, PASJ, 63, L37
Ziurys L. M., 1987, ApJ, 321, L81

This paper has been typeset from a TEX/LATEX file prepared by the author.